

TOWSHIP SELF NOISE CANCELLATION IN A TOWED SONAR ARRAY USING ADAPTIVE FILTERING

A. D. White* and D. Butler*.

(*)Plessey Naval Systems, Templecombe, Somerset.

1. INTRODUCTION

The limits on performance of sonar systems may, in many circumstances, be set by self noise levels. Adaptive noise cancellation (ANC) has been shown [Reference 1] to be useful for cancelling self noise in sensor outputs where a separate measurement of the offending noise source is available. An alternative to cancelling the noise at the sensor is to cancel it at the beamformer output. This may be more appropriate for systems where the number of beams is less than the number of hydrophones so that beamformer ANC is cheaper to implement. In this paper, therefore, we examine the improvements that can be made to target signal to noise ratio by using ANC techniques on a sonar beamformer output where self noise appears strongly in one beam and is used as a reference for cancelling the self noise in other beams. The self noise in these other beams is caused by sidelobes of these beams in the direction of the self noise source. These improvements will be seen to be a function of the relative levels of target field strength, ambient noise field strength and self noise strength as well as beamformer characteristics. Although general results are obtained we apply the results to the Plessey Naval Systems COMTASS towed array system as an example where self noise appears in many aft looking beams due to spatial aliasing of the tow ship noise coming primarily from a forward direction.

2. THEORY OF ADAPTIVE FILTERING OF BEAMFORMER OUTPUTS

2.1 Block Diagram Model

In Figure 1 $L(\omega)$, $H(\omega)$, $K(\omega)$ and $J(\omega)$ are the transfer functions between towship noise and target noise and forward and target beams.

$\sigma_{mm}(\omega)$ and $\sigma_{nn}(\omega)$ represent ambient noise in the two beams which is uncorrelated with both target and tow ship noise.

$\sigma_{xx}(\omega)$ is the power spectrum at the reference input to the adaptive filter.

$\sigma_{xd}(\omega)$ is the cross spectrum between reference and primary inputs of the adaptive filter.

The filter itself is an FIR filter whose weights, \underline{W} , are being adapted by the least mean squares (LMS) algorithm of Widrow (Reference 1).

We calculate the improvement, I , to the S/N ratio between the output and the primary input to the filter, subject to the condition that the filter has converged to its optimal value,

TOW SHIP SELF NOISE CANCELLATION

which is,

$$W'(\omega) = \frac{\sigma_{xd}(\omega)}{\sigma_{xx}(\omega)} \quad [\text{Reference 1, Chapter 10}]$$

where $W'(\omega)$ is the Fourier transform of \underline{W} .

$$\text{ie we want } I = \frac{\text{S/N output}}{\text{S/N primary}} \quad (1)$$

$$\text{subject to } W' = \frac{\sigma_{xd}(\omega)}{\sigma_{xx}(\omega)} = \frac{SLJ^* + UKH^*}{S|J|^2 + U|H|^2 + \sigma_{nn}} \quad (2)$$

where * denotes the complex conjugate, $S(\omega)$ is the target noise spectrum, $U(\omega)$ is the towship noise spectrum and the arguments have been omitted for clarity.

At the output, signal is given by:

$$S|_{\text{output}} = S|L - JW'|^2 \quad (3)$$

and noise is given by:

$$N|_{\text{output}} = U|K - HW'|^2 + \sigma_{nn}|W'|^2 + \sigma_{mm} \quad (4)$$

At the filter primary input, signal is given by:

$$S|_{\text{primary}} = S|L|^2 \quad (5)$$

and noise is given by:

$$N|_{\text{primary}} = U|K|^2 + \sigma_{mm} \quad (6)$$

Substituting (2), (3), (4), (5) and (6) into (1)

$$I = \frac{(U|K|^2 + \sigma_{mm})}{|L|^2} \left\{ \frac{|U(L|H|^2 - JKH^*) + L\sigma_{nn}|^2}{P + Q + R} \right\} \quad (7)$$

where $P = U|S(K|J|^2 - LHJ^*) + \sigma_{mm}K|^2$

$$Q = \sigma_{nn}|SLJ^* + UKH^*|^2$$

$$R = \sigma_{mm}|S|J|^2 + U|H|^2 + \sigma_{nn}|^2$$

TOW SHIP SELF NOISE CANCELLATION

Now substitute the conditions that:

i $L = H$ and $K = J$.

This corresponds to the target and tow ship being on their respective beam maximum response angles.

ii $\sigma_{mm} = \sigma_{nn} = 0$.

Ambient noise is zero represents the best possible performance that can be achieved with the beamformer/adaptive filter combination.

$$\text{Then } I = \frac{S/N \text{ output}}{S/N \text{ primary}} = \left(\frac{U}{S} \right)^2 \quad (8)$$

This very interesting result indicates that, under optimum conditions,

- i) the worse the S/N in the water, the greater is the noise cancellation by the adaptive filter, ie a -20dB S/N ratio in the water becomes a +20dB S/N ratio at the filter output.
- ii) the improvement is independent of the beamformer.

2.2 Beamformer Characteristics

We now develop the detailed equations for the signal to noise improvement by ANC which include the beamformer characteristics. The model assumes a constant amplitude plane wave self noise field coming from some forward direction and a constant amplitude plane wave target field, coming from another direction. These directions are not necessarily on beam axes. The ambient noise field is assumed to be uncorrelated with the target and self noise fields and also between pairs of sensors. The beamformer has been assumed to be full beam with shading. The power spectrum at the reference input to the ANC and the cross spectrum between reference and primary inputs of the ANC is calculated. The filter is assumed to have adapted to its optimum solution so that its output is minimised and its transfer function calculated from the two power spectra. The signal and noise at input and output of the ANC are then calculated using the optimised filter. Simplifications are then made that the shading is uniform and that the target and self noise sources lie on beam axes and the input and output signal to noise ratios are calculated. These are a complicated function of target, self noise and ambient fields strengths and transfer function between self noise and target beams. A further simplification is made that the ambient field strength is zero and the result of the earlier, simpler analysis (Section 2.1) that the improvement to the signal to noise ratio equals the square of the ratio of self noise to target field strengths is verified.

TOW SHIP SELF NOISE CANCELLATION

In the finite impulse response (FIR) LMS adapted filter of Figure 2, let $d(t)$ come from a beam looking towards a target and $x(t)$ from a beam looking towards a large noise source.

Let the array be a line of equally spaced elements, d apart, with weight a_n on element n .

Let $d(t)$ be the output of a beam steered to k_1 and $x(t)$ be the output of a beam steered to k_2 in Figure 3. The self noise field, $U(t)$, comes from direction k_u and the target field, $S(t)$, comes from direction k_s . There is additional ambient noise on each element which is assumed uncorrelated between elements.

The i th beam $y_i(t)$ is given by

$$y_i(t) = \sum_{n=1}^N a_n \{ S_n(t+T_i-n\tau_i) + U_n(t+T_i-n\tau_i) + m_n(t+T_i-n\tau_i) \} \quad (9)$$

where T_i is the arbitrary time reference
 τ_i is the steering delay between elements

and $s_n(t) = s(t+n\tau_s)$
 $u_n(t) = u(t+n\tau_u)$
 $m_n(t)$ is uncorrelated with s and u and $m_i, i \neq n$

Here τ_s = difference in arrival time of the target wavefront between elements.
 τ_u = difference in arrival time of the self noise wavefront between elements.

We find the autocorrelation function at the reference input $x(t)$ ($=y_2(t)$) and the cross correlation function between reference and primary input $d(t)$ ($=y_1(t)$) by forming

$$\begin{aligned} \phi_{xx}(\tau) &= \langle y_2(t+\tau)y_2(t) \rangle \\ \text{and } \phi_{xd}(\tau) &= \langle y_2(t+\tau)y_1(t) \rangle \end{aligned} \quad (10)$$

We take the Fourier transforms of (10) and calculate the output power spectrum (after adaptive cancellation)

$$\text{This is minimised when } W'(\omega) = \frac{\phi_{xd}^*(\omega)}{\phi_{xx}(\omega)}$$

TOW SHIP SELF NOISE CANCELLATION

Before substituting for $W'(\omega)$, signal and noise terms must be identified ie $W'(\omega)$ must be treated as a fixed filter determined from the statistical average properties of S , U and M . Thus the output signal is given by

$$\Phi_{oo}(\omega) = S(\omega) \{ |B_{s1}|^2 + |W(\omega)|^2 |B_{s2}|^2 - 2 \operatorname{Re}(W(\omega) e^{i\omega(T_2 - T_1)} B_{s1}^* B_{s2}) \}$$

where $S(\omega)$ is the target noise spectrum (transform of $\langle s(t+\tau) s(t) \rangle$) (11)

$$\text{and } B_{kl} = B(\theta_k, \theta_l; \omega) = \sum_{p=1}^N a_p^2 e^{\frac{i\omega d p}{c}} (\sin \theta_k - \sin \theta_l) \quad (12)$$

with k and l any of 1, 2, s, u

and the output noise is given by

$$\begin{aligned} \Phi_{nn}(\omega) = & U(\omega) \{ |B_{u1}|^2 + |W'(\omega)|^2 |B_{u2}|^2 - 2 \operatorname{Re}(W'(\omega) e^{i\omega(T_2 - T_1)} B_{u2} B_{u1}^*) \} \\ & + M(\omega) \{ \sum a_p^2 (1 + |W'(\omega)|^2) - 2 \operatorname{Re}(W'(\omega) e^{i\omega(T_2 - T_1)} B_{12}) \} \end{aligned} \quad (13)$$

where $U(\omega)$ and $M(\omega)$ are the towship spectrum and ambient noise spectrum respectively (transforms of $\langle u(t+\tau) u(t) \rangle$ and $\langle m(t+\tau) m(t) \rangle$).

$$\text{The input signal is given by } S(\omega) |B_{s1}|^2 \quad (14)$$

$$\text{The input noise is given by } U(\omega) |B_{u1}|^2 + M(\omega) \sum_{p=1}^N a_p^2 \quad (15)$$

If we simplify by substituting

$$\begin{aligned} a_i &= 1, i = 1, \dots, N && \text{(unshaded array)} \\ \theta_s &= \theta_1, \theta_u = \theta_2 && \text{(target and self noise on beam axes)} \end{aligned}$$

i) For $M(\omega) = 0$

$$I = \frac{(S/N)_{\text{out}}}{(S/N)_{\text{in}}} = \left(\frac{U}{S} \right)^2$$

ii) For $S(\omega) \ll U(\omega)$, $M(\omega)$ and $NU(\omega) \gg M(\omega)$

$$I = 1 + |B_{12}|^2 \frac{U(\omega)}{NM(\omega)}$$

TOW SHIP SELF NOISE CANCELLATION

3. THE PLESSEY NAVAL SYSTEM COMTASS TOWED ARRAY SYSTEM

This is a 32 hydrophone linear array with 1 metre spacing between unshaded hydrophones. Its normal frequency range is 400-1600 Hz. The data described here used only 28 of the channels (a tape recorder limitation) and the frequency range was limited to 400-1200 Hz. Figure 4 shows the output of beam 2 from the beamformer. This beam was steered towards the towship, a noisily run, non-military tugboat. Figure 5 shows the computed transfer function $|B_{12}|$ from tow-ship self noise acoustic field to one of the aft looking beams (beam 56) at an angle of -50.6° to broadside.

It should be compared with the COMTASS trials measured beam 56 output seen in Figure 6. Although the self noise spectrum from the tow ship was not flat the large lobe of self noise centred at about 860 Hz from the spatially aliased self noise spectrum is clearly seen. The frequency at which this noise is centred is steering delay or beam dependent. The shape of the curve in Figure 5 is identical to the frequency response from target power spectrum to reference beam ie at the aliasing frequency all of the target signal appears in the reference beam just as all of the tow ship self noise appears in the target beam.

Figure 6 also shows beam 56 after adaptive filtering with a 105 weight adaptive FIR. Clearly the main lobe and the smaller sidelobes are removed. Although these spectra are taken with 100 averages, the convergence speed of the filter used was sufficiently fast to follow the fast changing amplitude (>10 dB's in a few seconds) of the noise field. The theoretical spectrum of signal and noise before and after ANC is shown in Figure 7 for flat spectra into the array. The levels of self-noise, target and ambient levels are typical of a sonar environment. At the aliasing frequency, ~ 860 Hz, the normalised noise is cancelled but so is the target due to it appearing fully in the reference beam as well as the target beam. At this frequency, no target will be seen.

4. FILTER LENGTH, CAUSALITY AND CONVERGENCE RATE

In the analyses above, questions of the physical realizability of the adaptive filter were not considered. The expressions derived were ideal, based on the assumptions of an infinitely long, two-sided (non-causal) adaptive FIR filter that has finished adapting to its final optimal solution. Such a filter cannot in reality be implemented, but its performance can be closely approximated.

The length of the filter required in this application depends on the sample rate and the length of the impulse response from self noise field to target beam. This latter depends in turn on the steering delay. It is simple to show that the length of filter required for beam space cancellation for beams aft of broadside is given by $(N-1)(\tau_u + \tau_s)$

where τ_u = forward looking beam steering delay
 τ_s = target beam steering delay

TOW SHIP SELF NOISE CANCELLATION

The delay required in the primary input to the filter in order to make the relationship between primary and reference inputs causal is given by $(N-1) \tau_0$.

The last assumption that the filter has adapted to its final optimal solution can only be approximately true when used with non-stationary data. The ideal filter is a complicated function of target strength, self noise strength and ambient noise strength. As these change the filter must adapt sufficiently quickly to follow the changing conditions. The adaption rate can be increased by increasing a convergence parameter in the adaption algorithm, however the penalty here is that too fast a convergence results in too high a level of misadjustment noise (Reference 1). A compromise must be found that allows the filter to adapt at a fast enough rate to follow the non-stationary data and yet minimise misadjustment noise. This has been achieved with the COMTASS data. The recorded tow ship self noise data varies in amplitude over several seconds while the target and ambient field strengths can be assumed to vary over a similar time scale. The convergence parameter used in the COMTASS data experiments was such that the filter had essentially fully converged in under a second. Thus the ANC tracks the changing conditions without a significant level of misadjustment noise.

For the data described above, beam 56 at an angle of -50.6° to broadside, for 28 sensors spaced 1m apart, the length of filter calculated was 102 weights at a sample rate of 3072 Hz and a primary delay of 56 samples. In order to allow for tolerances of components etc, the actual filter length used was 105 weights with primary delay 57 samples.

5. THE MOTOROLA DSP56001 REAL-TIME ADAPTIVE NOISE CANCELLER

The Motorola DSP56001 is a fourth generation, low power, HCMOS, user programmable digital signal processor. The core of the processor consists of three execution units - the Data Arithmetic and Logic Unit (ALU), the address ALU and the Program Controller, which operate in parallel. The architecture has been designed to maximise throughput in data intensive applications. This has enabled the FIR filter calculation (Reference 1) to be carried out in three machine cycles per weight and the weight update calculation in 6 machine cycles per weight. The clock rate is 20.5 MHz. Thus the processor is fast enough to handle the filtering and adaption of more than 100 weights between samples at the 3072 Hz sampling rate used for the experiments on the COMTASS sea trials data.

TOW SHIP SELF NOISE CANCELLATION

Calculations indicate that this processor can adapt 256 weights with the Widrow LMS algorithm at a sample rate of up to about 10 kHz. Longer filters than this can be implemented at a lower sample rate but this means using off-chip RAM for storage of weights and data. For sonar applications where different frequency bands use different sample rates and with many beams requiring ANC, the processing load becomes large. Thus many processors will be required. For submarines, where there are severe limitations on space and heat generation by evermore electronics, the present generation of digital signal processors, of which the MOTOROLA 56001 is one, may not be adequate. Thus we expect future applications of ANC to be implemented in very high performance IC's (VHPIC).

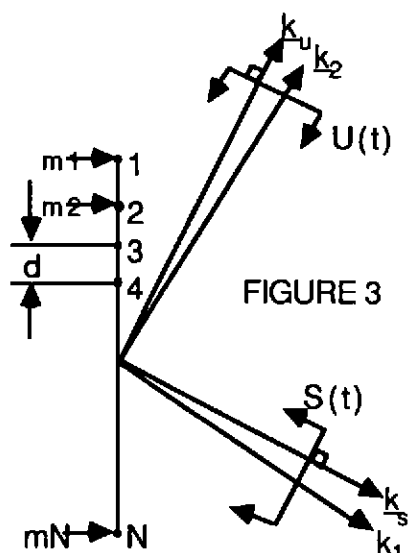
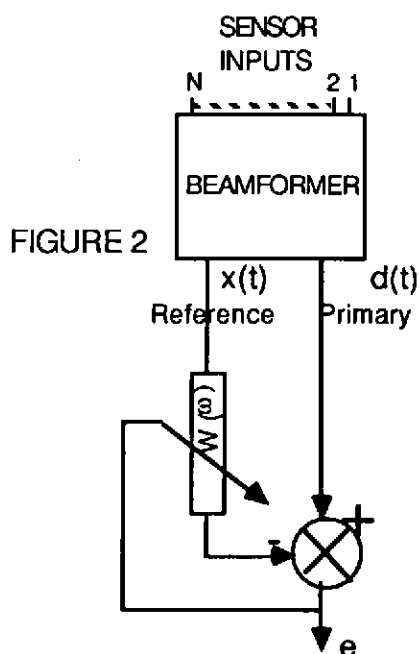
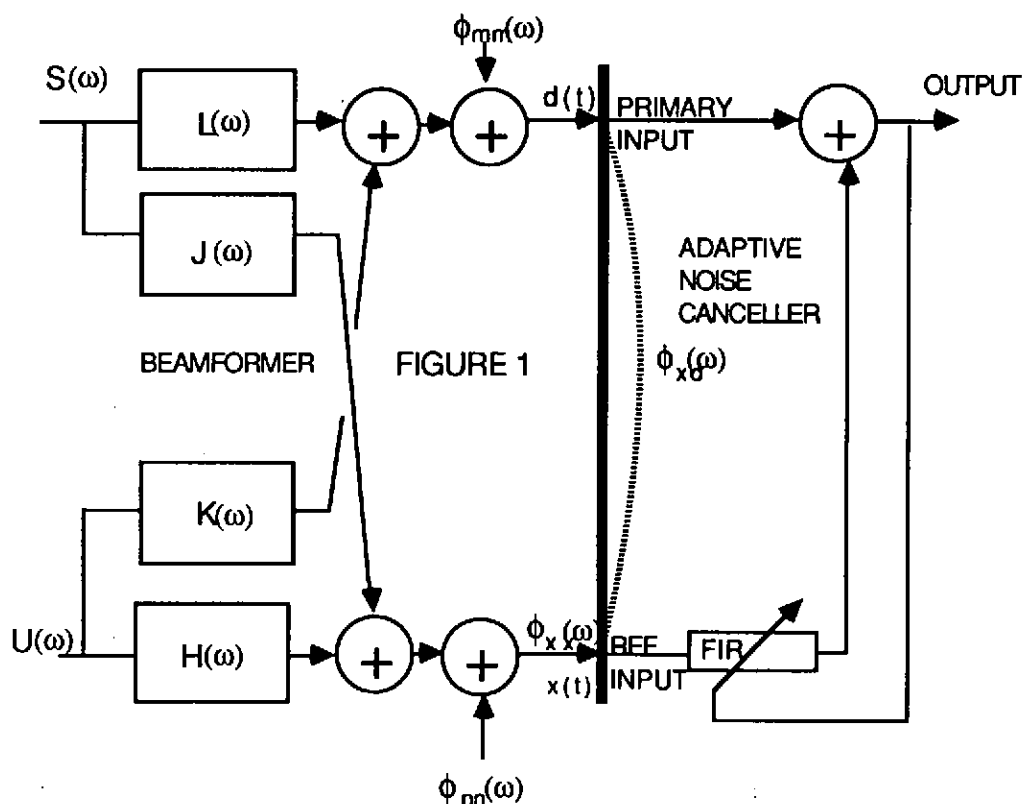
6. CONCLUSIONS

We have demonstrated, both theoretically and experimentally in real-time on COMTASS sea trials data, the improvements that can be made to the signal to noise ratio at the output of a beamformer by adaptive noise cancellation (ANC). Numerically, the improvement is a function of tow ship self noise field strength, target field strength and ambient sea noise field strength. Beamformer characteristics also affect the degree of improvement. In realistic conditions, where the ratios of self noise to ambient noise, and ambient noise to target strength are greater than unity the improvements can be considerable. Where the target strength is greater than the self noise, the S/N ratio will be made worse although, of course, in this unlikely situation, S/N improvement is not necessary.

Reference

1. "Adaptive Signal Processing". B. Widrow, S. Stearns. Prentice Hall. 1985.

TOW SHIP SELF NOISE CANCELLATION



TOW SHIP SELF NOISE CANCELLATION

FIGURE 4. Beam 2. Towship spectrum

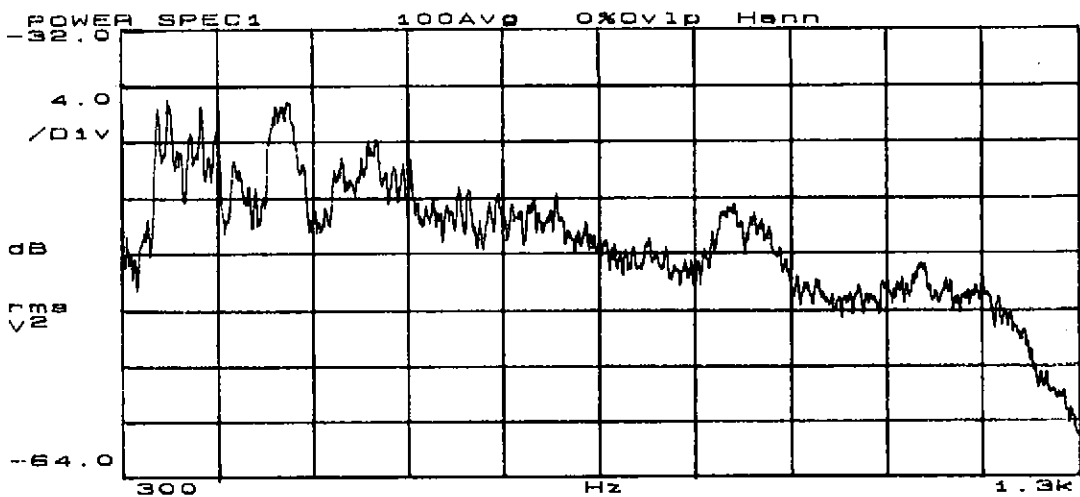
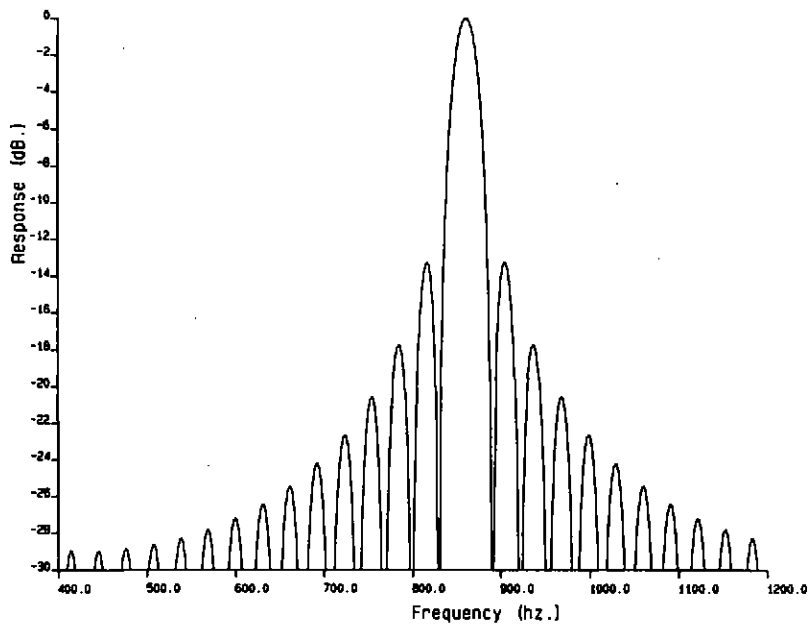


Figure 5. Frequency response towship spectrum to target beam 56.



TOW SHIP SELF NOISE CANCELLATION

FIGURE 8. Beam 56 before and after ANC

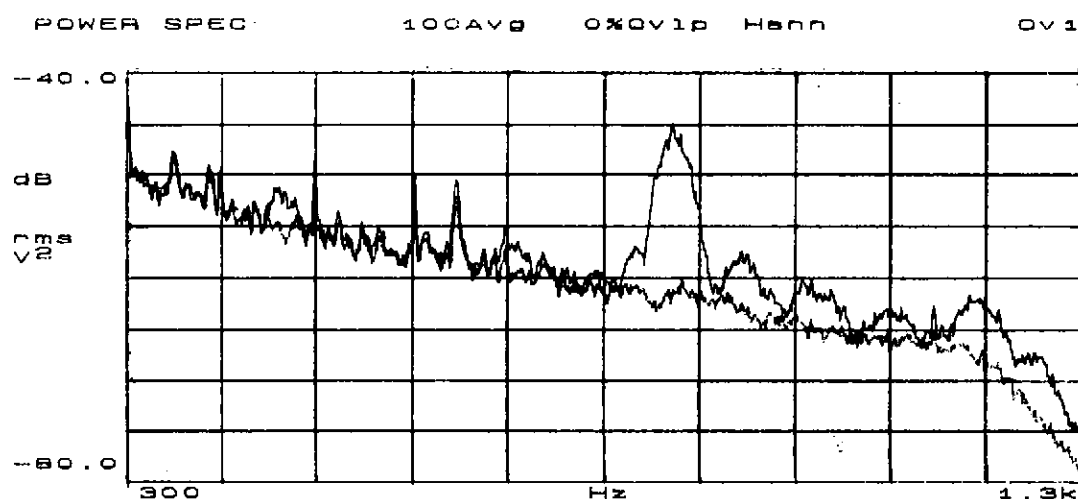
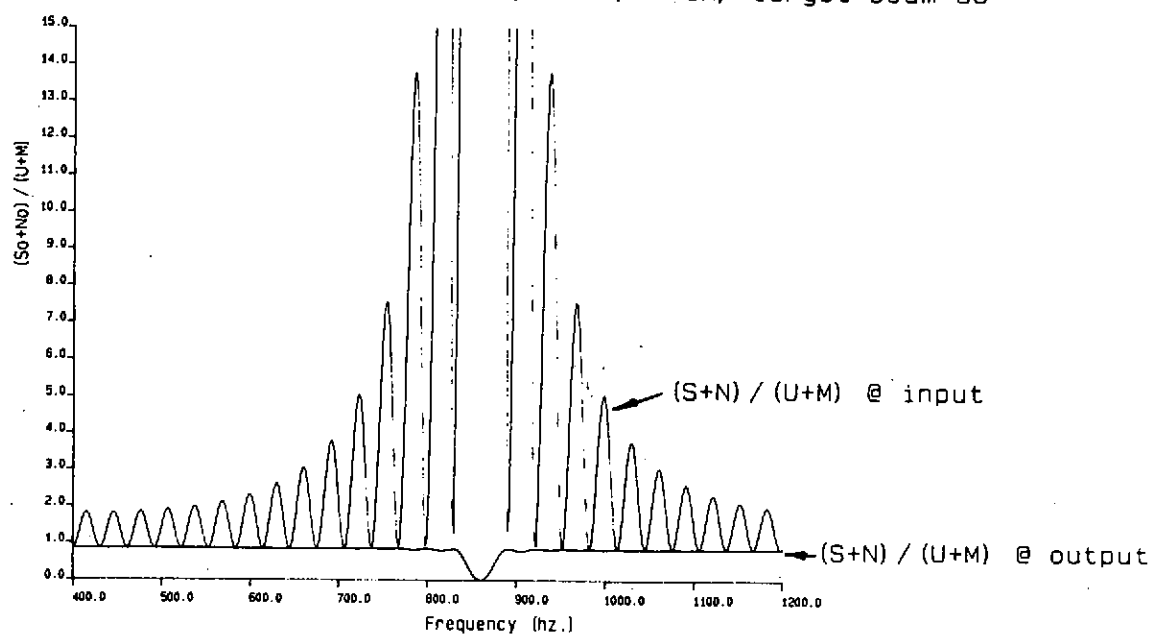


Figure 7 Signal and noise at the input and output
of an adaptive noise canceller (target and beam on axis)
 $U=50$, $M=1$, $S=0.02$, $N=28$, $d=1m$, target beam=56



A VERSATILE LOW FREQUENCY SONAR TRANSMITTER

Wood W.J., Griffiths J.W.R. and Zhang J.
University of Technology, Loughborough, UK.

Summary

A 16 channel sonar transmitting system working at a frequency of about 4.5 kHz has been developed. Each channel is driven by a linear high power amplifier capable of supplying 1 kW to each element and the inputs to the amplifiers are derived from a digital signal processor. The system is similar in principle to the 40 kHz system which has already been developed at the University but the method of signal generation is entirely new. The paper describes the details of the system together with some early measurements of its performance.

Introduction

A very successful versatile transmitting system built at the University has already been reported. (Refs 1,2). The primary frequency for this system is around 40 kHz but with the large power transmitted it is also possible to use the system in the parametric mode and hence generate low frequency signals. Although such a system has many advantages as have been described in the references the process generating the low frequencies in the water is very inefficient with the result that the effective source levels are rather low compared to the source level at the primary frequency. It was thus decided to build a low frequency system operating at a primary frequency of about 4 kHz but at the same time taking the opportunity to try a new method of signal generation.

Signal Generation

In the 40 kHz system the required digital signals are generated by a dedicated Nascom Computer and then stored in a set of 16 memories. The contents of the memories are read out in parallel through D/A converters to each of the power amplifiers and so to the staves of the array. At the time this system was developed memories were much more expensive than at present and hence to save memory only 4 bits per sample was used. The generation of the required signals by the computer is relatively slow and when a different set of signals are required this takes some time. Thus for the new system it was decided to look for a higher resolution per sample and for a more versatile solution.

There are many possible processors that could have been used and to some extent the decision is more dependent on local expertise and easy availability. The availability of an IBM-PC plug-in board based on the Motorola DSP56001 led to the use of this processor for the initial experiments.

A block diagram is shown in figure 1. A separate board carries out the D/A conversion (using 12 bits) and filtering for each channel. This system is able to generate 16 separate sinewaves whose frequency and phase may be controlled so as to provide many different modes of operation. Essentially a look up table containing sine wave samples is successively accessed to produce the required waveforms.

Transducer Array

Low frequency transducers, by virtue of the fact that they are quite large, are inherently less susceptible to the slight misalignments that degrade the performance of the higher frequency units. As such, an array of low frequency elements, tends to be well matched and more predictable. Tests on the elements bought for this project (Massa Type TR-1061A) showed that they were indeed well matched and that their performance was very good. This matching means that experiments that rely on the predictability of the array e.g., sidelobe reduction by amplitude shading, should prove more successful. The frequencies and impedances at resonance were very consistent and as can be seen from the typical transmitter sensitivity curve in figure 2 the bandwidth of the devices was fairly wide, increasing the flexibility of the system.

An array of 16 elements was constructed as a line array with a spacing of 180 mm which is approximately 0.5 lambda at the centre frequency.

Transmitter Amplifiers

Each transducer is capable of handling 500 Watts of electrical power at a duty cycle of 20%, and each needs its own power amplifier. It was decided to make use of the dual 1 kW units that had been specifically developed for use with the 40 kHz flexible transmitter. Minor adjustments enabled them to operate at the lower frequency, and new output transformers were wound to match the amplifiers to the transducers. However the transformers were responsible for some loss of performance in the purity of the output waveform.

Deployment and Testing.

The array consists of a steel frame 3 m long, containing sixteen elements each weighing 7.5 kg giving a total weight of about 260 kg and because of its size it was not possible to do any substantial testing of the array in the departmental tank which is only approximately 9m x 6m x 2m deep. The far field of the array (operating at 4.4 kHz) is about 24 m, and although focussing could have been used the relatively long period for a signal of these frequencies limits the number of cycles of acoustic signal that could be received before multipath interference occurs, particularly from reflections from the surface and the bottom of the tank.

Initial tests have been carried out at a nearby reservoir in Derbyshire where the water is up to 30 m deep and a reasonable depth is maintained for a distance of over 1 km in a straight line from the test point at the 'draw-off' tower. The tower stands away from the dam wall and is connected to it by a permanent concrete bridge. Because of the size of the array and the difficulty in rotating it about an axis normal to its length it was decided to hang the array vertically. A winch mechanism with associated aluminium pole sections enabled the array to be held rigidly in a vertical position.

To obtain the beampattern in the plane of the line array a hydrophone can be lowered through the sound field making suitable geometric corrections. Initial experiments made use of an existing 'hydrophone pole' arrangement. The hydrophone cable was free to move through a series of 'eyes' attached to the pole enabling the hydrophone to be moved through the vertical sound field. Using this arrangements measurements could be made up to a maximum distance of 7.6 m from the array face which although still within the near field, allowed initial experiments to be performed.

Initial Results

In the appendix it is shown that the theoretical source level for the system is approximately 228 dB ref. 1 μ P at 1 m. There is some slight uncertainty about this figure since the directivity index and efficiency for the individual elements are not known exactly. The measured value referred back to 1m is 227 dB ref. 1 μ P.

Figure 3 shows the theoretical vertical beam pattern for a 14 element array focussed at 7.5 m i.e., well inside the near field and the points on the curve show the measured values. The agreement between the theoretical near field pattern and the results of the practical measurement although not excellent is encouraging.

The expected waveform which would be received by a hydrophone in the far field can be simulated in the laboratory simply by adding the outputs from all the channels from the signal generator using a resistor combining network. Figure 4.1 shows such a trace in which the beam is being swept across the sector using the sector scanning techniques discussed in earlier work and it can be seen that the beam has the expected $\sin(nx)/\sin(x)$ form. In figure 4.2 we see the waveform on the hydrophone placed at 7.5 m and of course because this is within the nearfield the beam is not properly formed. However by suitably phasing the channel outputs the beam can be focussed at this distance and in figure 4.4 we see the resulting waveform. It is now forming a beam similar to the expected unfocussed far field result. It is interesting to note that the output from the resistor combination, seen in figure 4.3, which represents the anticipated far field waveform is in this case itself unfocused and is similar to the original unfocussed beam shown figure 4.1.

Figure 5 shows the theoretical pattern for a ripple fire and in figure 6 we see the result obtained from the hydrophone.

Conclusions

A versatile transmitting system working at 4.5kHz has been developed and the early trials show that it is performing as expected.

Acknowledgement

This work has been carried out with the support of Procurement Executive Ministry of Defence.

References

1. Goodson A.D. et al. 'A High Power Flexible Sonar Transmitter', Proc I.E.R.E. Conf. on "Electronics in Ocean Technology, Edinburgh, March 1987.
2. Cook J.C. et al. 'Sector Scanning Sonar Using Transmitter Scanning', Proc. Conf. UDT1988, London Oct. 1989

Appendix. Calculation of Source level

Area of array at centre frequency is

$$16\lambda \text{ by } 0.5\lambda = 8\lambda^2$$

and hence the Directivity Index is approximately 20 dB

$$\text{Acoustic Power} = 0.6 \times 16 \times 500 = 4800 \text{ W}$$

$$\text{SL} = 10 \log(4800) + \text{DI} + 171$$

$$= 228 \text{ dB ref. } 1 \mu\text{P at } 1 \text{ m}$$

FIG 1. SCHEMATIC DIAGRAM OF SIGNAL GENERATOR

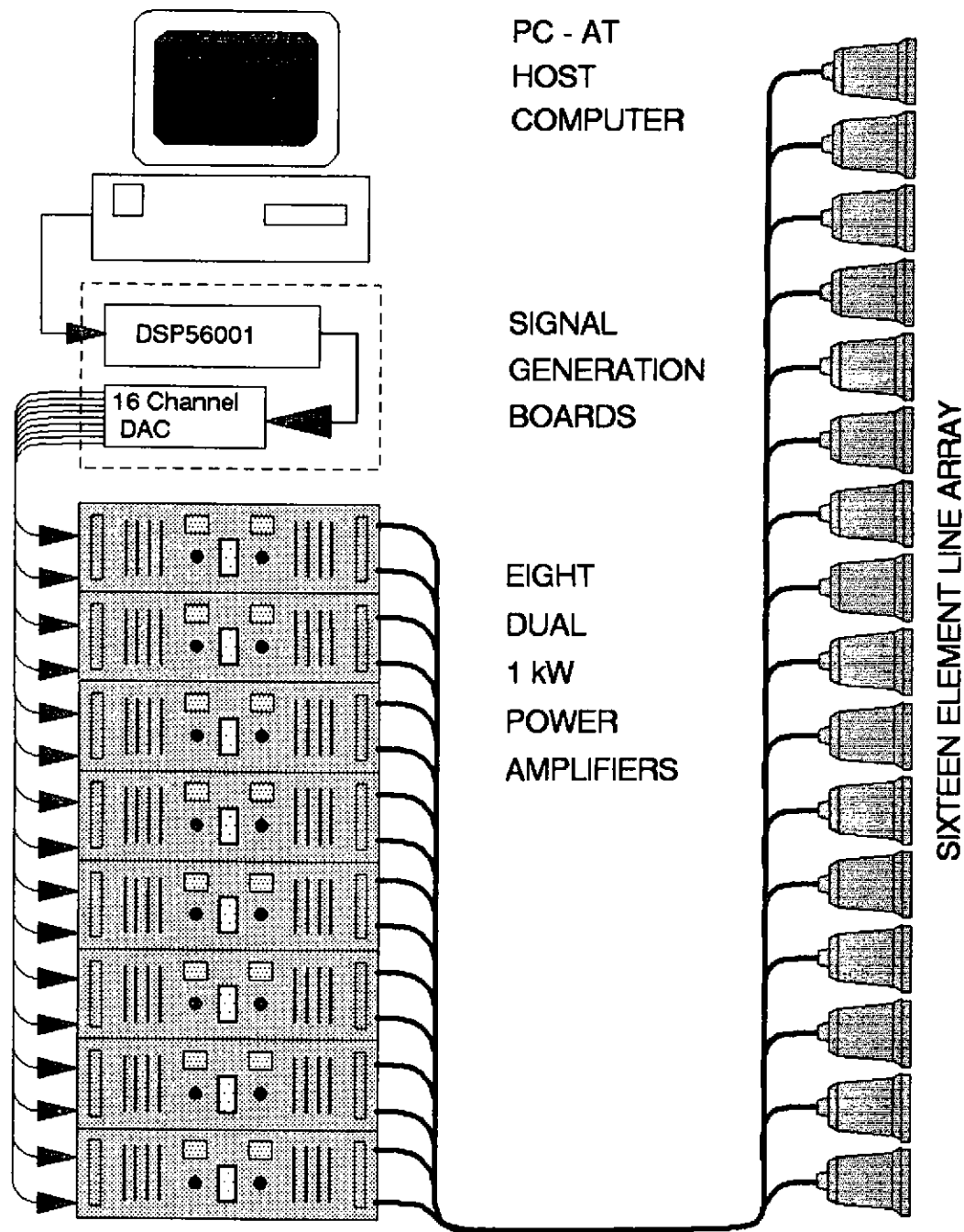


FIG 2. ELEMENT TRANSMIT SENSITIVITY CURVE

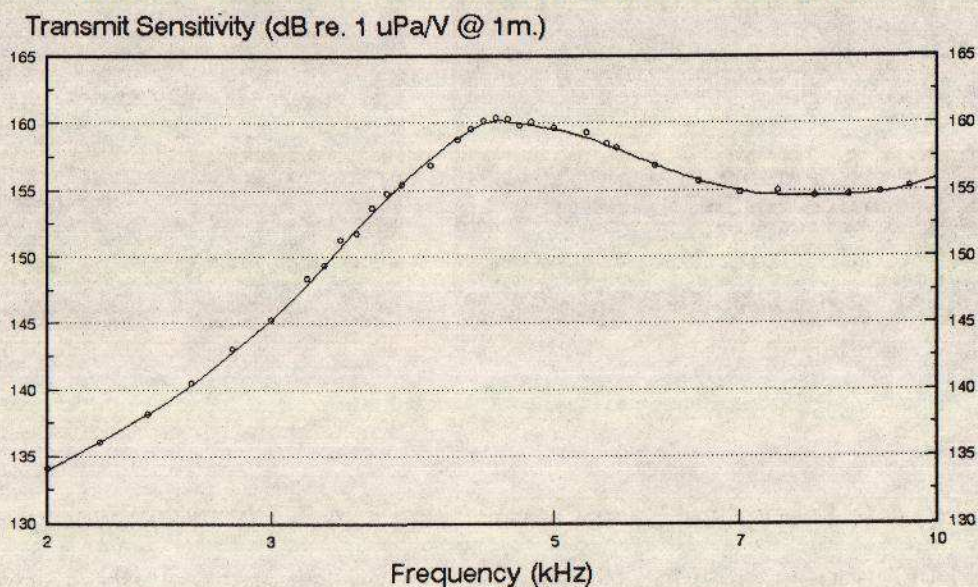
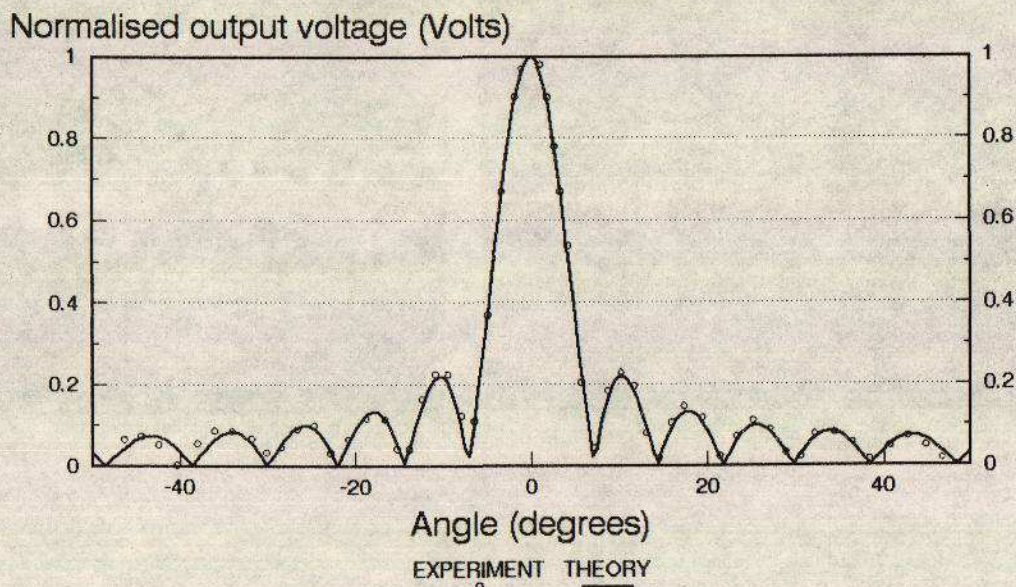


FIG 3. VERTICAL BEAMPATTERN

14 Elements - 4.65 kHz



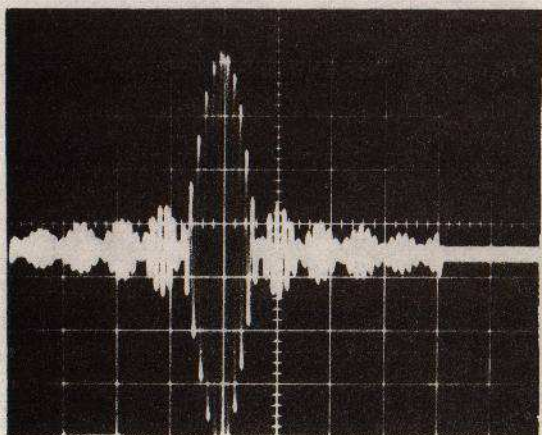


Fig 4.1 Theoretical Swept Beam
14 Channels +45 to -45 degrees
(0.2 V / Div. 2 mS / Div)

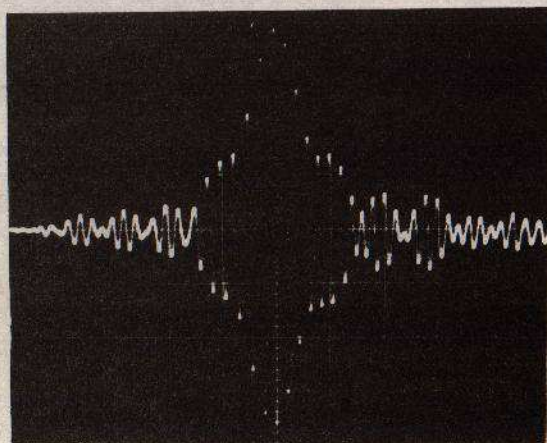


Fig 4.2 Practical Swept Beam
14 Elements +45 to -45 degrees
(0.5 V / Div. 1 mS / Div)

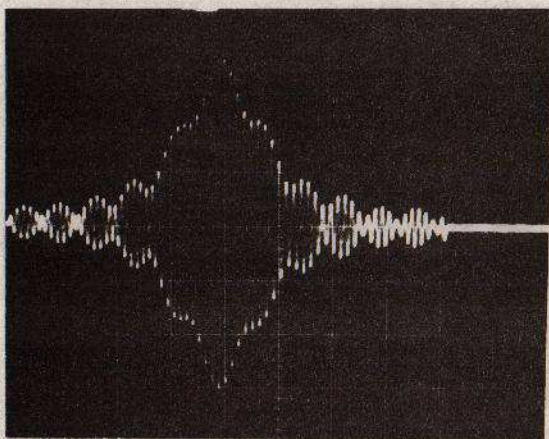


Fig 4.3 Focussed Sweep (Theory)
14 Channels +45 to -45 degrees
(0.2 V / Div. 2 mS / Div.)

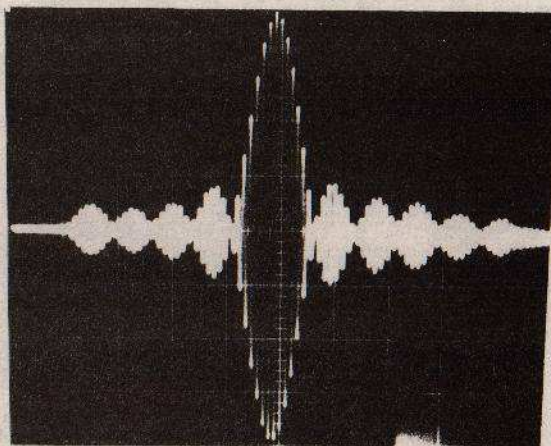


Fig 4.4 Focussed Sweep (Expt.)
14 Elements +45 to -45 degrees
(0.55 V / Div. 2 mS / Div.)

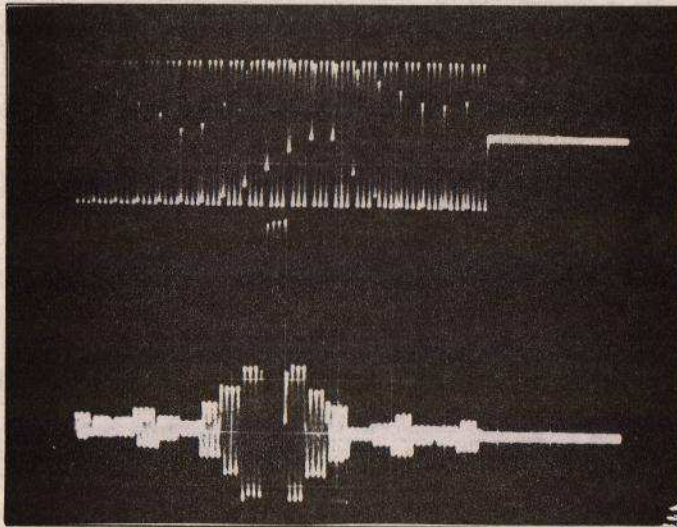


Figure 5
Ripple Beam (Theory)
14 Channels
+45 to -45 degrees
(0.2V/Div 2mS/Div)
Also single channel o/p

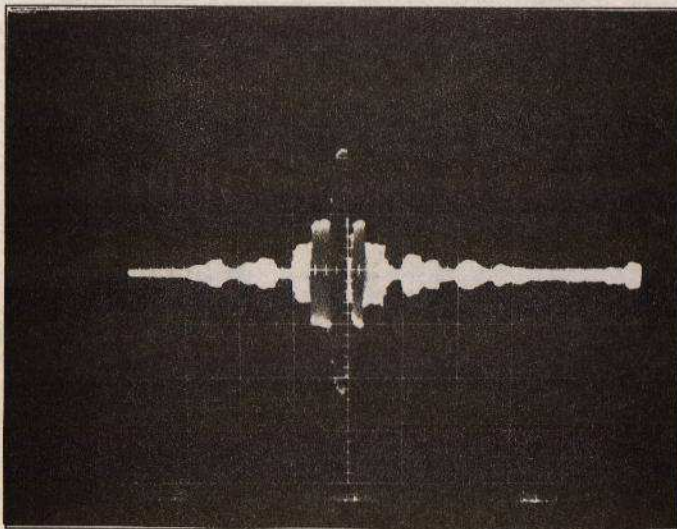


Figure 6
Ripple Beam (Expt.)
14 Elements
+45 to -45 degrees
Focussed at 7.5 m.
(1V/Div 5mS/Div)